Electrical Power and Energy Systems 55 (2014) 179–186

Contents lists available at ScienceDirect

Electrical Power and Energy Systems

journal homepage: www.elsevier.com/locate/ijepes

Optimal placement of dispatchable and nondispatchable renewable DG units in distribution networks for minimizing energy loss

Duong Quoc Hung [a], N. Mithulananthan [a,*], Kwang Y. Lee [b]

[a] School of Information Technology and Electrical Engineering, University of Queensland, Brisbane, QLD 4072, Australia
[b] Department of Electrical and Computer Engineering, Baylor University, Waco, TX 76798-7356, USA

ARTICLE INFO

Article history:
Received 1 July 2013
Received in revised form 3 September 2013
Accepted 6 September 2013

Keywords:
Distributed generation
Dispatchable DG
Energy loss
Nondispatchable DG
Optimal power factor operation
Renewable energy

ABSTRACT

This paper presents a methodology for the integration of dispatchable and nondispatchable renewable distributed generation (DG) units for minimizing annual energy losses. In this methodology, analytical expressions are first proposed to identify the optimal size and power factor of DG unit simultaneously for each location for minimizing power losses. These expressions are then adapted to place renewable DG units for minimizing annual energy losses while considering the time-varying characteristics of demand and generation. A combination of dispatchable and nondispatchable DG units is also proposed in this paper. The proposed methodology has been applied to a 69-bus test distribution system with different scenarios. The results demonstrate that dispatchable DG units or a combination of dispatchable and nondispatchable DG units can lead to a substantial reduction in annual energy losses when compared to nondispatchable DG units. The results also show that a maximum annual energy loss reduction is achieved for all scenarios proposed with DG operation at optimal power factor.

1. Introduction

With the concern on depleting fossil fuel resources and environmental concerns, renewable distributed generation (DG) units such as biomass, wind and solar are emerging as an alternative energy solution. DG owners usually receive incentives from utilities by setting a high selling energy price [1]. From the utility perspective, DG units located close to distribution system loads can lead to power flow reduction, loss minimization, voltage profile enhancement, voltage stability improvement, network upgrade deferral, etc. [2–21], DG units can participate into the competitive market to provide ancillary services such as spinning reserve, voltage regulation, reactive power control and frequency control [22–24]. However, the high penetration of intermittent renewable resources (i.e., wind and solar) together with demand variations has introduced many challenges to distribution systems such as power fluctuations, voltage rise and high losses [1].

The optimal DG placement and sizing issues for minimizing power and energy losses in distribution networks have attracted great attention in recent years. Most of the researchers have focused on developing methodologies for minimizing power losses with the assumption that DG units are dispatchable and allocated at the peak demand [25]. Typical examples for such works are analytical approaches [4–8], a numerical method [9], and a wide range of heuristic algorithms: Simulated Annealing (SA) [10], Genetic Algorithm (GA) [11], Particle Swarm Optimization (PSO) [12,13], Artificial Bee Colony Algorithm (ABC) [14], Modified Teaching–Learning Based Optimization (MTLBO) [15], and Harmony Search Algorithm (HSA) [16]. However, such approaches may not solve a practical case of time-varying demand and renewable generation (e.g., nondispatchable wind output) as the optimum DG size at the peak demand may not remain at other loading levels. Hence, the energy loss minimization may not be optimal. Recently, a few studies on renewable DG integration for minimizing energy losses have been reported while considering the time-varying characteristics of both demand and generation. For example, wind DG units are sized using a GA-based approach [17] and an optimal power flow-based method [18]. In [19], different types of renewable DG unit (i.e., biomass, wind and solar PV) are located and sized using analytical approaches. In [20], the optimal location and size of wind DG units are addressed using a probabilistic-based planning approach. This approach has also been employed in [21] for locating and sizing different types of nondispatchable renewable DG units. So far, a combination of dispatchable and nondispatchable DG placement for minimizing energy losses has not been reported in the literature. On the other hand, most of the studies presented above have assumed that DG units operate at pre-specified power factor (usually unity power factor). In these researches, only the location and size have been considered, while the optimal power factor for each DG unit that would be a crucial part for minimizing energy losses has been neglected. Depending on the

* Corresponding author. Tel.: +61 7 3365 4194; fax: +61 7 3365 4999.
E-mail address: mithulan@itee.uq.edu.au (N. Mithulananthan).

0142-0615/$ - see front matter © 2013 Elsevier Ltd. All rights reserved.
http://dx.doi.org/10.1016/j.ijepes.2013.09.007

characteristics of loads served, each DG unit that can deliver both active and reactive power at optimal power factor may have positive impacts on energy loss reduction.

This paper first proposes analytical expressions to determine the optimal size and power factor of DG unit simultaneously for each location for minimizing power losses. These analytical expressions are obtained by improving the work in [7], where the analytical expressions were developed to calculate different types of DG unit when the DG power factor is pre-specified. The proposed analytical expressions are then adapted to allocate dispatchable and nondispatchable DG units to minimize energy losses while considering the time-varying characteristics of demand and generation. Moreover, a combination of dispatchable and nondispatchable renewable DG units is proposed. Here, DG unit is considered as a dispatchable source (e.g., biomass), if its output can be adjusted, whereas DG unit is considered as a nondispatchable source (e.g., wind), if its output cannot be adjusted.

The rest of the paper is structured as follows: Section 2 describes the modeling of load and renewable DG. Section 3 introduces a methodology to accommodate renewable DG sources for minimizing energy losses. Section 4 portrays a 69-bus test distribution system along with numerical results and discussions. Finally, Section 5 summaries the contribution of the work.

2. Load and renewable resources modeling

2.1. Load modeling

The system considered in this work is assumed to follow the load curve of the IEEE-RTS system in Fig. 1 [26]. As shown in the figure, each year is divided into four seasons (winter, spring, summer and fall). An hourly load curve of a day is representing each season. The load curve of four 24-h days (24 × 4 = 96 h) is subsequently representing the four seasons in a year (8760 h). The seasonal maximum and minimum in load demand occurred during summer and fall, respectively. With a peak demand of 1 p.u., the load factor (*LF*) or average load level of the system can be defined by (1) as the ratio of the area under the load curve in p.u. to the total duration.

$$LF = \sum_{t=1}^{96} \frac{\text{p.u. } load(t)}{96} \tag{1}$$

2.2. Renewable resources modeling

Biomass and wind sources are assumed to utilize technologies that can operate at any desired power factor. Biomass DG unit is modeled as a synchronous machine and wind DG unit uses doubly-fed induction generators or full converter synchronous machines. Biomass DG unit is assumed to be a dispatchable source which can be dispatched according to the load curve as shown in Fig. 1. In this case, the capacity factor (*CF*) of biomass unit is equal to the *LF* as given in Eq. (1). On the other hand, wind DG unit is assumed to be a nondispatchable source following the output curve for each season per year [27], as depicted in Fig. 2. It is noted that different wind patterns could be easily incorporated in the proposed methodology below. As shown in Fig. 2, a year is divided into four seasons. An hourly generation output pattern for a day is representing each season. The generation output curve of four 24-h days (24 × 4 = 96 h) is then representing the four seasons in a year (8760 h). The seasonal maximum and minimum in wind power availability occurred during winter and summer, respectively. With a peak of 1 p.u., the *CF* of wind DG unit is defined by (2) as the ratio of the area under the output curve in p.u. to the total duration.

$$CF = \sum_{t=1}^{96} \frac{\text{p.u. DG } output(t)}{96} \tag{2}$$

2.3. Scenarios

In order to demonstrate the effectiveness of the proposed approach, the following four scenarios have been considered:

- Scenario#1: No DG unit.
- Scenario#2: Dispatchable biomass DG units.
- Scenario#3: Nondispatchable wind DG units.
- Scenario#4: A combination of dispatchable biomass and nondispatchable wind DG units as a dispatchable source.

Here, the assumption is that wind DG unit is nondispatchable and owned by developers and controlled by distribution network operators (DNOs). Biomass DG unit is dispatchable and owned and operated by DNOs.

3. Proposed methodology

3.1. Power and energy losses

The total active power loss in a distribution system with *N* buses as a function of active and reactive power injections at all buses can be calculated as follows [28]:

$$P_{loss} = \sum_{i=1}^{N}\sum_{j=1}^{N}[\alpha_{ij}(P_iP_j + Q_iQ_j) + \beta_{ij}(Q_iP_j - P_iQ_j)] \tag{3}$$

where $\alpha_{ij} = \frac{r_{ij}}{V_iV_j}\cos(\delta_i - \delta_j)$; $\beta_{ij} = \frac{r_{ij}}{V_iV_j}\sin(\delta_i - \delta_j)$; $V_i\angle\delta_i$ is complex voltage at bus *i*; $r_{ij} + jx_{ij} = Z_{ij}$ is the *ij*th element of $[Z_{bus}]$ impedance matrix; P_i and P_j are active power injections at buses *i* and *j*, respectively; Q_i and Q_j are reactive power injections at buses *i* and *j*, respectively.

As shown in Fig. 1, each year has four seasons. A load curve for a 24-h day is representing each season. The load curve of four 24-

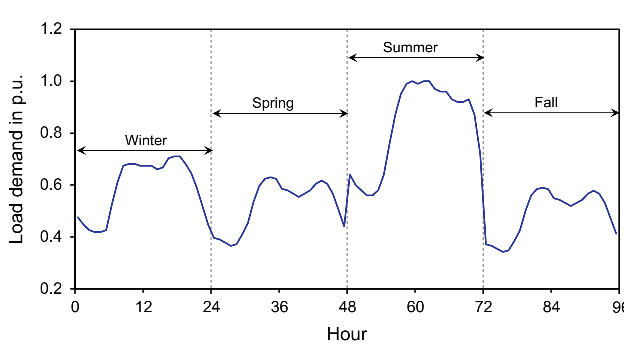

Fig. 1. Hourly load demand curve.

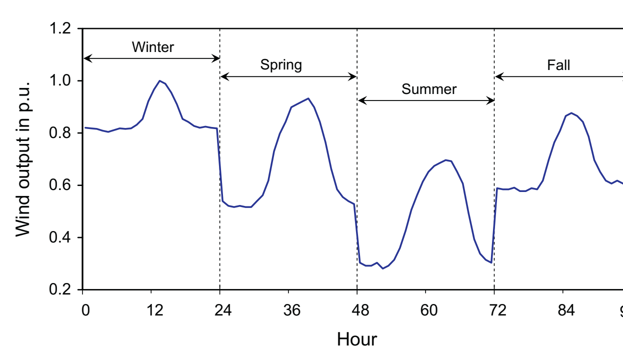

Fig. 2. Hourly wind output curve.

h days ($24 \times 4 = 96$ h) is subsequently representing the four seasons in a year. The total number of hours per year is 365×24 (8760) h. Therefore, the 96-h load curve is repeated 91.25 times to represent 1 year ($91.25 \times 96 = 8760$). Here, 96 h in four seasons a year are corresponding to 96 periods (load levels). The active power loss, P^t_{loss}, at each period t is obtained from (3). Hence, the total *annual* energy loss in a distribution system with a time duration (Δt) of 1 h can be expressed as:

$$E_{loss} = 91.25 \sum_{t=1}^{96} P^t_{loss} \Delta t \tag{4}$$

3.2. Analytical expression for sizing DG unit with a predefined power factor at various locations [7]

This section briefly describes an analytical expression developed in [7] to calculate different types of DG unit for minimizing power losses when the DG power factor is pre-specified. Here, the active and reactive power injections at bus i where DG unit is installed are respectively given as:

$$P_i = P_{DGi} - P_{Di} \tag{5}$$

$$Q_i = Q_{DGi} - Q_{Di} = a_i P_{DGi} - Q_{Di} \tag{6}$$

where $Q_{DGi} = a_i P_{DGi}$, P_{DGi} and Q_{DGi} are respectively the active and reactive power injections from DG unit at bus i, $a_i = (sign)\tan(\cos^{-1}(pf_{DGi}))$ with {$sign = +1$: DG unit injecting reactive power, $sign = -1$: DG unit consuming reactive power}; P_{Di} and Q_{Di} are respectively the active and reactive power of load at bus i; pf_{DGi} is the operating power factor of DG unit at bus i.

Substituting Eqs. (5) and (6) into Eq. (3), we obtain the total active power loss with DG unit as follows:

$$P_{loss} = \sum_{i=1}^{N}\sum_{j=1}^{N} \begin{bmatrix} \alpha_{ij}((P_{DGi} - P_{Di})P_j + (a_i P_{DGi} - Q_{Di})Q_j) \\ +\beta_{ij}((a_i P_{DGi} - Q_{Di})P_j - (P_{DGi} - P_{Di})Q_j) \end{bmatrix} \tag{7}$$

The total active power loss can reach a minimum value if the partial derivative of Eq. (7) with respect to the active power injection from DG at bus i (P_{DGi}) is zero.

$$\frac{\partial P_{loss}}{\partial P_{DGi}} = 2\sum_{j=1}^{N}[\alpha_{ij}(P_j + a_i Q_j) + \beta_{ij}(a_i P_j - Q_j)] = 0 \tag{8}$$

Eq. (8) can be rearranged as follows:

$$\alpha_{ii}(P_i + a_i Q_i) + X_i + a_i Y_i = 0 \tag{9}$$

where

$$X_i = \sum_{\substack{j=1 \\ j\neq i}}^{N} (\alpha_{ij}P_j - \beta_{ij}Q_j); \quad Y_i = \sum_{\substack{j=1 \\ j\neq i}}^{N} (\alpha_{ij}Q_j + \beta_{ij}P_j)$$

Substituting Eqs. (5) and (6) into Eq. (9), we obtain Eq. (10) which is used to calculate the optimal size of different types of DG unit at bus i for minimizing power losses when the DG power factor (pf_{DGi}) or value a_i is known. This expression can be written as [7]:

$$P_{DGi} = \frac{\alpha_{ii}(P_{Di} + a_i Q_{Di}) - X_i - a_i Y_i}{\alpha_{ii}(a_i^2 + 1)} \tag{10}$$

3.3. Proposed analytical expressions for calculating the optimal size and power factor at various locations

This section proposes analytical expressions based on an improvement to the work in [7] mentioned in Section 3.2 to determine the optimal size and power factor of DG unit simultaneously for each location. Here, the total active power loss is minimum if the partial derivative of Eq. (7) with respect to variable a_i (or pf_{DGi}) becomes zero.

$$\frac{\partial P_{loss}}{\partial a_i} = 2\sum_{j=1}^{N}[\alpha_{ij}Q_j + \beta_{ij}P_j] = 0 \tag{11}$$

Eq. (11) can be rearranged as follows:

$$\alpha_{ii}Q_i + Y_i = 0 \tag{12}$$

Substituting Eq. (6) into Eq. (12), we get:

$$a_i = \frac{1}{P_{DGi}}\left(Q_{Di} - \frac{Y_i}{\alpha_{ii}}\right) \tag{13}$$

The relationship between the power factor of DG (pf_{DGi}) and variable a_i at bus i can be expressed as:

$$pf_{DGi} = \cos(\tan^{-1}(a_i)) \tag{14}$$

Finally, the optimal P_{DGi} and its pf_{DGi} for the total system loss to be minimum can be obtained from (10), (13), and (14) as follows:

$$P_{DGi} = P_{Di} - \frac{X_i}{\alpha_{ii}} \tag{15}$$

$$pf_{DGi} = \cos\left(\tan^{-1}\left(\frac{\alpha_{ii}Q_{Di} - Y_i}{\alpha_{ii}P_{Di} - X_i}\right)\right) \tag{16}$$

3.4. Computational procedure

Scenario 1: Run load flow for each period (or load level) of the day and find the total annual energy loss using Eq. (4).

Scenario 2: Fig. 3 shows an example of the output curve of a single dispatchable biomass DG unit for the 69-bus system [29], as described in Section 4.1, in four seasons. This curve follows the load demand pattern in Fig. 1 and was obtained using a computational procedure as follows:

Step 1: Run base case load flow at the peak load level for the year and find the total power loss using Eq. (3).

Step 2: Find the optimal location, size and power factor of DG unit at the peak load level for the year.

- (a) Find the optimal size $\left(P^{peak}_{DGi}\right)$ and the optimal power factor using Eqs. (15) and (16), respectively.
- (b) Place DG unit obtained earlier at each bus, one at a time. Calculate the power loss for each case using Eq. (7).
- (c) Locate the optimal bus at which the power loss is minimum with the corresponding optimal size or maximum output (P^{max}_{DG}) at that bus.

Step 3: Find the optimal DG output at the optimal location for period t as follows, where p.u. *load*(t) is the load demand in p.u. at period t.

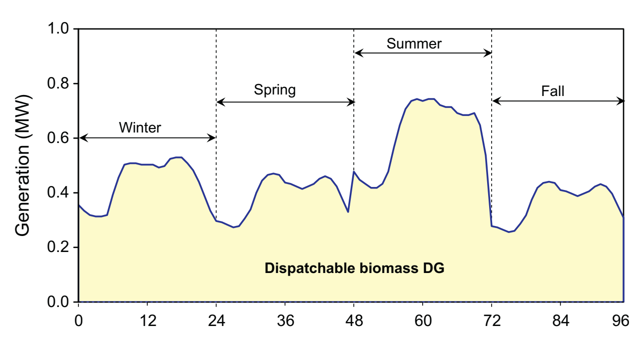

Fig. 3. Hourly optimal generation curve of biomass DG unit.

$$P^t_{DG} = \text{p.u. } load(t)P^{max}_{DG} \quad (17)$$

Step 4: Run load flow with each DG output obtained in *step* 3 for each period, find the total energy loss using Eq. (4), and repeat *steps* 2–4. Stop if any of the following occurs and the previous iteration solution is obtained.
(a) the bus voltage at any bus is over the upper limit;
(b) the branch current is over the upper limit;
(c) the total DG size is larger than the system demand plus loss;
(d) the maximum number of DG units are unavailable.

Scenario 3: Fig. 4 shows an example of the output curve of a single nondispatchable wind DG unit for the 69-bus system [29], as described in Section 4.1, in four seasons. This curve follows the wind output pattern in Fig. 2 and was obtained using a computational procedure as follows:

Step 1: Run load flow for the system without DG unit at the average load level for the year or at the load factor as given in Eq. (1) and find the total power loss using Eq. (3).
Step 2: Find the optimal location, size and power factor of DG unit at the average load level for the year.
(a) Find the optimal size (P^{avg}_{DGi}) and the optimal power factor using Eqs. (15) and (16), respectively.
(b) Place DG unit obtained earlier at each bus, one at a time. Calculate the power loss for each case using Eq. (7).
(c) Locate the optimal bus at which the power loss is minimum with the corresponding optimal size at the average load level or the average output (P^{avg}_{DG}) at that bus.
Step 3: Find the capacity factor (*CF*) of wind DG unit based on its daily output curve using Eq. (2).
Step 4: Find the optimal DG size or maximum DG output at the optimal location as follows:

$$P^{max}_{DG} = \frac{P^{avg}_{DG}}{CF} \quad (18)$$

Step 5: Find the optimal DG output at the optimal location for period *t* as follows, where p.u. DG *output*(*t*) is the DG output in p.u. at period *t*.

$$P^t_{DG} = \text{p.u. DG } output(t)P^{max}_{DG} \quad (19)$$

Step 6: Run load flow with each DG output obtained in *step 5* for each period, find the total energy loss using Eq. (4), and repeat *steps* 2–6. Stop if any of the following occurs and the previous iteration solution is obtained.
(a) the bus voltage at any bus is over the upper limit;
(b) the branch current is over the upper limit;
(c) the total DG size is larger than the system demand plus loss;
(d) the maximum number of DG units are unavailable.

When the power factor of DG unit is pre-specified, the computational procedure is similar to the above with exception that the optimal DG size for each bus is determined using Eq. (10) rather than Eq. (15).

Scenario 4: Fig. 5 shows an example of the output curve of a dispatchable and nondispatchable DG mix for the 69-bus system [29], as described in Section 4.1, in four seasons. This curve follows the demand profile in Fig. 1 and was obtained using the computational procedure as explained below. Here, the wind output pattern in Fig. 5 follows the wind output curve in Fig. 2 on the condition that wind penetration is in its maximum. Biomass DG units are utilized as an additional dispatchable source to fill up the supply energy portion that wind DG units cannot. Notice that the total DG output in MW for each period in scenario 4 (a mix of one dispatchable DG unit and one nondispatchable DG unit) is the same as that in scenario 2 (one dispatchable DG unit) on the condition that nondispatchable DG penetration is in its maximum.

Step 1: Find the optimal location, size and power factor of DG unit and the corresponding total energy loss using the computational procedure in scenario 2.
Step 2: Select the optimal location and power factor of dispatchable and nondispatchable DG units as calculated in *step* 1.
Step 3: Find the optimal size or maximum output of nondispatchable DG unit (P^{max}_{DG}) over all periods on the condition that its output is no more than that of DG unit as specified in *step* 1, at each period.
Step 4: Find the optimal output of nondispatchable DG unit for period *t* as given in Eq. (19).
Step 5: Calculate the output of dispatchable DG unit that is equal to the output of DG unit in *step* 1 minus the output of nondispatchable DG unit in *step* 4, for each period; then find the optimal size or maximum output of dispatchable DG unit over all periods.

4. Case study

4.1. Test systems

The proposed methodology has been applied to an 11 kV 69-bus radial distribution system, as depicted in Fig. 6. The complete system data at the peak load demand are given in [29]. This system is supplied from two substations with a total peak load of 4.47 MW and 3.06 MVar. The total system power loss at the peak demand without DG connection is 227.53 kW.

4.2. Assumptions and constraints

The lower and upper voltage thresholds should be 0.94 p.u. and 1.06 p.u., respectively, and the feeder thermal limits are 5.1 MVA (270 A).

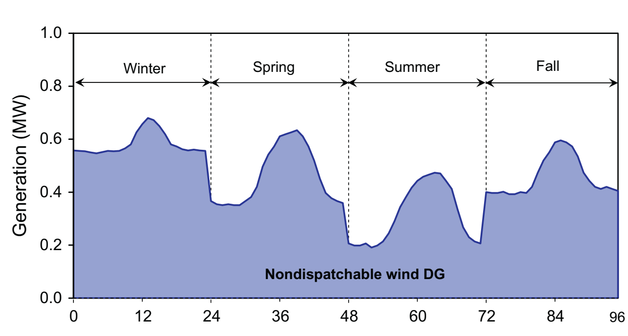

Fig. 4. Hourly optimal generation curve of nondispatchable wind DG unit.

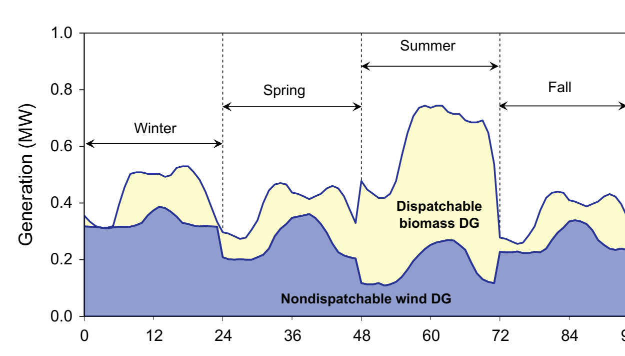

Fig. 5. Hourly optimal generation curve of wind–biomass DG mix.

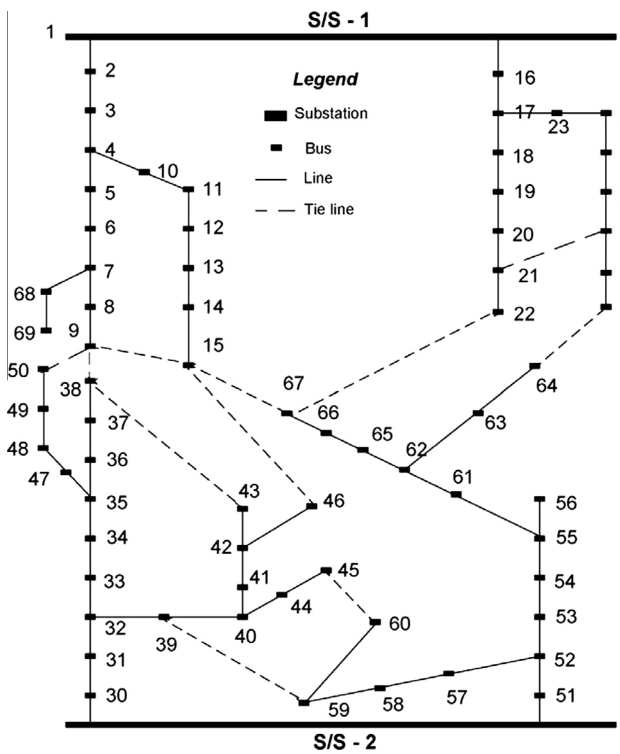

Fig. 6. Single line diagram of the 69-bus test distribution system.

The demand of the system is assumed to follow the load curve in Fig. 1 [26]. Wind DG units are assumed to be nondispatchable and follow the wind output curve in Fig. 2, but different wind patterns could be easily incorporated in the proposed methodology.

Biomass DG units are assumed to be allocated at any bus in the system. The locations of wind DG units may be identified by resources and geographic factors. As their sites are unspecified in the test system, they are assumed to be installed at any bus. However, when the locations are pre-specified, the optimal sizes and power factors with the lowest corresponding power loss can be quickly determined based on the proposed methodology. The power factor of DG units remains unchanged over all periods. The number of DG units is predefined at two for scenarios 2 and 3, and at four for scenario 4. However, the proposed methodology can consider the different number of DG units.

4.3. DG placement without considering power factor limit

Fig. 7 shows the hourly load demand and power loss curves of the system in four seasons a year in scenario 1. The load demand curve shown in Fig. 7 follows the hourly load demand curve in Fig. 1. The peak demand occurred at the period 59 in summer, whereas the lowest demand was at the period 77 in fall. The significant power losses were observed at periods in summer. The total annual energy import from the grid without DG unit is calculated as tracing the area under Fig. 7 times 91.25 days. In this case, the total annual energy import is found at 24.556 GW h, which is a sum of the total system load demand (23.787 GW h) and the total system energy loss (0.769 GW h).

Without considering the power factor limit, Figs. 8–10 show the optimal output curves of DG units in four seasons in scenarios 2, 3 and 4, respectively, and the power import from the grid. For scenario 2, the total output of biomass DG units at each period (Fig. 8) is dispatched following the demand curve (Fig. 7). Similarly, for scenario 4, the total output of biomass-wind DG units at each

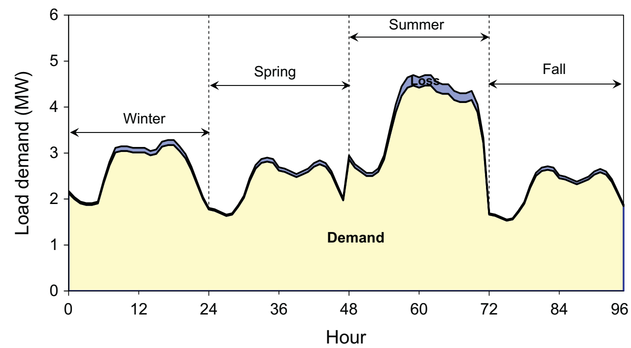

Fig. 7. Hourly load demand and power loss curves (scenario 1).

period in Fig. 10 is also dispatched according to the demand curve in Fig. 7. Here, the wind output pattern in Fig. 10 follows the wind output curve in Fig. 2 on the condition that wind penetration is in its maximum. Biomass DG units are utilized as an additional dispatchable source to fill up the supply energy portion that wind DG units cannot. As the total DG output patterns of scenarios 2 and 4 are the same and are dispatched following the load demand in Fig. 7, the power loss at each period in scenario 2 is identical to that in scenario 4 as depicted in Fig. 11. On the other hand, as wind DG units in scenario 3 (Fig. 9) cannot dispatch following the demand pattern in Fig. 7, the power loss at each period in scenario 3 is higher than that in scenarios 2 and 4 as shown in Fig. 11. In addition, it can be revealed from Figs. 8–10 that the integration of DG units amounts to the reduction in the total energy import from the grid in all scenarios, resulting from the DG energy production and system energy loss reduction.

Table 1 shows a summary and comparison of the simulation results obtained for four different scenarios with and without DG units in the 69-bus system. For scenarios 2–4 with DG units, the results include the type of DG units and the location, size and power factor for each type. The annual energy loss and its loss reduction for each scenario are also presented in this table. The optimal locations of DG units for each scenario are identified at buses 62 and 35 with the corresponding sizes and power factors as shown in the table. A significant energy loss reduction is observed in scenarios 2–4 (with DG units) when compared to scenario 1 (without DG units). In scenarios with DG units, the highest loss reduction is found in scenarios 2 and 4, while the lowest loss reduction is obtained in scenario 3. The combination of dispatchable and nondispatchable DG units in scenario 4 can yield the same loss reduction as dispatchable biomass DG units in scenario 2. Notice that the optimal DG power factors at buses 62 and 35 are different at 0.79 and 0.83 (lagging), respectively.

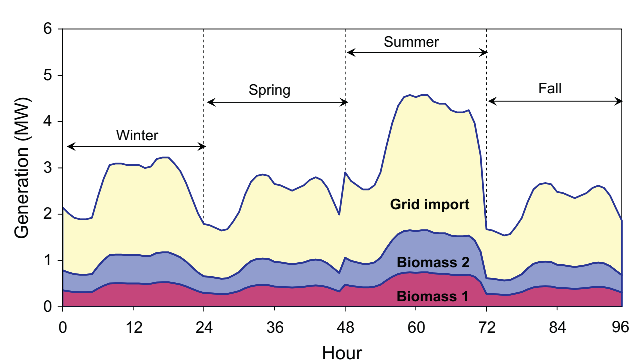

Fig. 8. Hourly optimal generation curve of biomass DG units (scenario 2).

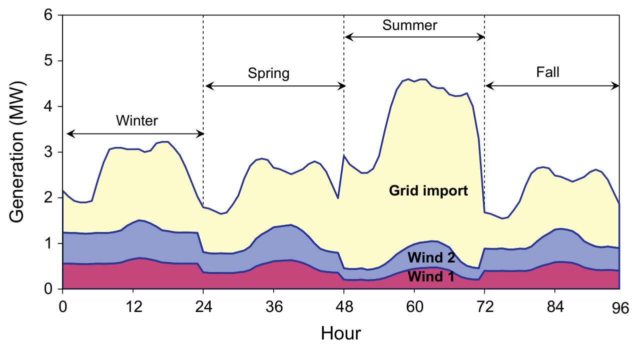

Fig. 9. Hourly optimal generation curve of wind DG units (scenario 3).

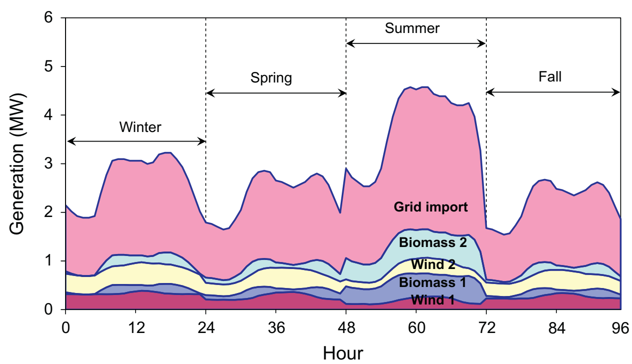

Fig. 10. Hourly optimal generation curve of wind-biomass DG mix (scenario 4).

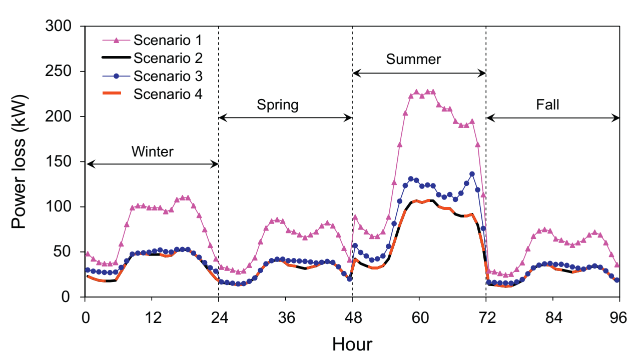

Fig. 11. Hourly power loss curve in scenarios 1–4.

4.4. Biomass versus wind

Fig. 12 shows the power loss reduction over 96 periods in four seasons in scenarios 2–4. It is obvious that scenario 2 can produce a maximum loss reduction over each period because the biomass output was dispatched according to the varying demand curve.

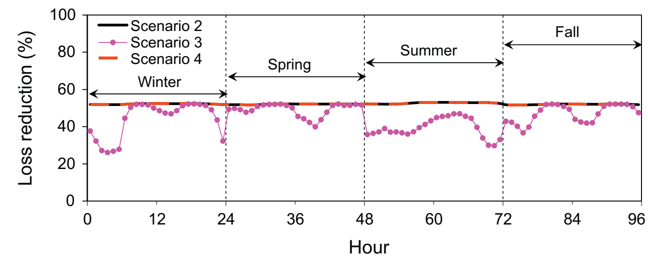

Fig. 12. Hourly percentage power loss reduction in scenarios 2–4.

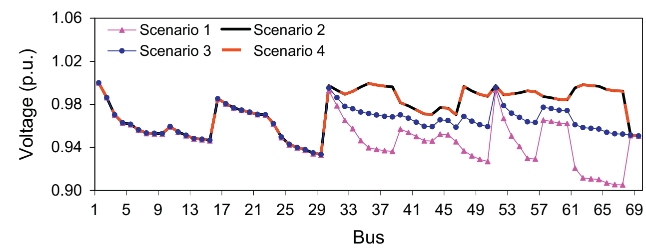

Fig. 13. Voltage profile at extreme periods (period 59) for scenarios 1–4.

On the other hand, the maximum loss reduction is found at a few periods in scenario 3 although the wind DG output cannot be dispatched according to the varying demand curve. Scenario 4 can yield the same loss reduction as scenario 2. The advantage is that biomass DG units have capability to dispatch according to load demand. Consequently, scenarios 2 and 4 that include dispatchable biomass DG units are superior to scenario 3 from the perspective of total annual energy loss reduction as shown in Fig. 12.

4.5. Voltage profiles

Fig. 13 shows the voltage profiles for scenarios 1–4 at the extreme periods (load levels) where the voltage profiles are the worst. In the absence of DG units, the extreme period is at the peak period 59 as depicted in Fig. 7, at which the voltages at some buses are under 0.94 p.u. In the presence of DG units, by considering the combination of the demand and DG output curves, the extreme periods are also at the peak period 59 for scenarios 2–4, as shown in Figs. 8–10. It can be observed from the figure that after DG units are integrated at the extreme periods, the voltage profiles improve significantly. It is interesting to note that the voltage profiles in scenario 2 (dispatchable DG units) or scenario 4 (a mix of dispatchable and nondispatchable DG units) are better than those in scenario 3 (nondispatchable DG units).

It is worth noting that the optimal size and location of DG units obtained for power loss minimization using the proposed method are in close agreement with the results of recently published methods such as heuristic [30], PSO [12,31], SA [10], ABC [14], MTLBO [15], and HSA [16].

Table 1
Optimal DG placement results for different scenarios without considering power factor limit.

Scenarios	1	2 (biomass)		3 (wind)		4 (wind–biomass mix)			
DG type	No DG	Bio 1	Bio 2	Wind 1	Wind 2	Wind 1	Bio 1	Wind 2	Bio 2
Location (bus)		62	35	62	35	62	62	35	35
Size (MVA)		0.94	0.99	0.86	0.99	0.49	0.71	0.56	0.82
Power factor (lagging)		0.79	0.83	0.79	0.83	0.79	0.79	0.83	0.83
Annual loss (MW h)	768.50		365.38		426.92				365.38
Loss reduction (%)			52.46		44.45				52.46

Table 2
Optimal DG placement results for different scenarios considering power factor limit.

Scenarios	1	2 (biomass)		3 (wind)		4 (wind-biomass mix)			
DG type	No DG	Bio 1	Bio 2	Wind 1	Wind 2	Wind 1	Bio 1	Wind 2	Bio 2
Location (bus)		62	35	62	35	62	62	35	35
Size (MVA)		0.89	1.05	0.81	0.96	0.44	0.67	0.52	0.79
Power factor (lagging)		0.95	0.95	0.95	0.95	0.95	0.95	0.95	0.95
Annual loss (MW h)	768.50		401.41		458.04				401.41

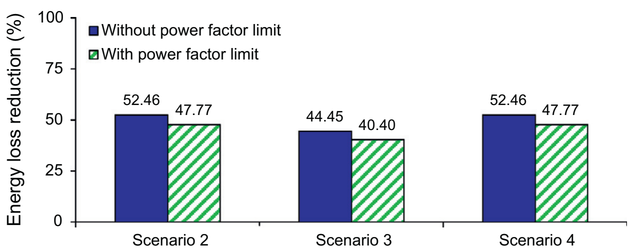

Fig. 14. Impact of the power factor of DG units on energy loss reduction.

4.6. Impact of power factors of DG unit on energy losses

As reported in [32], the grid codes of many countries require that grid-connected wind turbines should provide the capability of reactive power control or power factor control in a specific range. For instance, in the Ireland, the power factor of wind turbines is required to be from 0.835 leading to 0.835 lagging. It should be from 0.95 leading to 0.95 lagging in Italy and the United Kingdom. Hence, in this study, the power factor is limited in the range of 0.95 leading and 0.95 lagging to assess the impact of the power factor of DG units on energy losses. Table 2 summarizes and compares the results of DG placement for four different scenarios with and without DG units in the 69-bus system considering the power factor limit from 0.95 leading to 0.95 lagging. For each scenario with DG units, the results include the type, location, size, power factor and corresponding energy loss. The optimal locations of DG units for each scenario are identified at buses 62 and 35 with the corresponding sizes as shown in Table 2. In this case, the best power factor of all DG units is found to be at 0.95 lagging. However, the optimal power factor of DG units are 0.79 and 0.83 (lagging), at buses 62 and 35, respectively, when the power factor limit was not considered as shown in Table 1. It is revealed that imposing the power factor limit has a negative impact on the energy loss reduction at a maximum difference of nearly 5% when compared to the case without considering the power factor limit, as presented in Fig. 14. However, this may depends on the characteristics of the system and DG output.

5. Conclusion

This paper has presented a methodology to determine the optimal location, size and power factor of dispatchable and nondispatchable renewable DG units for minimizing annual energy losses. In this methodology, analytical expressions are first proposed to determine the optimal size and power factor of DG unit simultaneously for each location to minimize power losses. These expressions are then adapted to locate and size different renewable DG units and calculate the optimal power factor for each unit to minimize energy losses while considering the time-varying characteristics of demand and generation. Moreover, a combination of dispatchable and nondispatchable renewable DG units is proposed in this paper. The proposed methodology has been applied to different renewable DG scenarios with and without power factor limit for a 69-bus test distribution system. The results show that dispatchable DG units or a combination of dispatchable and nondispatchable DG units can minimize annual energy losses significantly when compared to nondispatchable DG units alone. The results also indicate that a maximum annual energy loss reduction has been obtained for all scenarios proposed with DG operation at optimal power factor. It is also revealed that imposing power factor limit can result in an increase in annual energy losses from the optimal value.

References

[1] Omran WA, Kazerani M, Salama MMA. Investigation of methods for reduction of power fluctuations generated from large grid-connected photovoltaic systems. IEEE Trans Energy Convers 2011;26:318–27.
[2] Hedayati H, Nabaviniaki SA, Akbarimajd A. A method for placement of DG units in distribution networks. IEEE Trans Power Del 2008;23:1620–8.
[3] Ettehadi M, Ghasemi H, Vaez-Zadeh S. Voltage stability-based DG placement in distribution networks. IEEE Trans Power Del 2013;28:171–8.
[4] Wang C, Nehrir MH. Analytical approaches for optimal placement of distributed generation sources in power systems. IEEE Trans Power Syst 2004;19:2068–76.
[5] Gözel T, Hocaoglu MH. An analytical method for the sizing and siting of distributed generators in radial systems. Electr Power Syst Res 2009;79:912–8.
[6] Acharya N, Mahat P, Mithulananthan N. An analytical approach for DG allocation in primary distribution network. Int J Electr Power Energy Syst 2006;28:669–78.
[7] Hung DQ, Mithulananthan N, Bansal RC. Analytical expressions for DG allocation in primary distribution networks. IEEE Trans Energy Convers 2010;25:814–20.
[8] Murthy VVSN, Kumar A. Comparison of optimal DG allocation methods in radial distribution systems based on sensitivity approaches. Int J Electr Power Energy Syst 2013;53:450–67.
[9] Chang RW, Mithulananthan N, Saha TK. Novel mixed-integer method to optimize distributed generation mix in primary distribution systems. In: Proceedings of the Australasian Universities power engineering conference, Brisbane, Australia, 25–28 September, 2011.
[10] Injeti SK, Prema Kumar N. A novel approach to identify optimal access point and capacity of multiple DGs in a small, medium and large scale radial distribution systems. Int J Electr Power Energy Syst 2013;45:142–51.
[11] Akorede MF, Hizam H, Aris I, Ab Kadir MZA. Effective method for optimal allocation of distributed generation units in meshed electric power systems. IET Gener Transm Distrib 2011;5:276–87.
[12] AlRashidi MR, AlHajri MF. Optimal planning of multiple distributed generation sources in distribution networks: a new approach. Energy Convers Manage 2011;5:3301–8.
[13] Kansal S, Kumar V, Tyagi B. Optimal placement of different type of DG sources in distribution networks. Int J Electr Power Energy Syst 2013;53:752–60.
[14] Abu-Mouti FS, El-Hawary ME. Optimal distributed generation allocation and sizing in distribution systems via artificial bee colony algorithm. IEEE Power Del 2011;26:2090–101.
[15] Martín García JA, Gil Mena AJ. Optimal distributed generation location and size using a modified teaching–learning based optimization algorithm. Int J Electr Power Energy Syst 2013;50:65–75.
[16] Rao RS, Ravindra K, Satish K, Narasimham SVL. Power loss minimization in distribution system using network reconfiguration in the presence of distributed generation. IEEE Trans Power Syst 2013;28:317–25.
[17] Ugranlı F, Karatepe E. Optimal wind turbine sizing to minimize energy loss. Int J Electr Power Energy Syst 2013;53:656–63.
[18] Ochoa LF, Harrison GP. Minimizing energy losses: optimal accommodation and smart operation of renewable distributed generation. IEEE Trans Power Syst 2011;26:198–205.
[19] Hung DQ, Mithulananthan N, Bansal RC. Analytical strategies for renewable distributed generation integration considering energy loss minimization. Appl Energy 2013;105:75–85.

[20] Atwa YM, El-Saadany EF. Probabilistic approach for optimal allocation of wind-based distributed generation in distribution systems. IET Renew Power Gener 2011;5:79–88.
[21] Atwa YM, El-Saadany EF, Salama MMA, Seethapathy R. Optimal renewable resources mix for distribution system energy loss minimization. IEEE Trans Power Syst 2010;25:360–70.
[22] Mashhour E, Moghaddas-Tafreshi SM. Bidding strategy of virtual power plant for participating in energy and spinning reserve markets – Part I: Problem formulation. IEEE Trans Power Syst 2011;26:949–56.
[23] Rueda-Medina AC, Padilha-Feltrin A. Distributed generators as providers of reactive power support – a market approach. IEEE Trans Power Syst 2012;28:490–502.
[24] Yuen C, Oudalov A, Timbus A. The provision of frequency control reserves from multiple microgrids. IEEE Trans Ind Electron 2011;58:173–83.
[25] Georgilakis PS, Hatziargyriou ND. Optimal distributed generation placement in power distribution networks: models, methods, and future research. IEEE Trans Power Syst 2013;28:3420–8.
[26] Pinheiro JMS, Dornellas CRR, Schilling MT, Melo ACG, Mello JCO. Probing the new IEEE reliability test system (RTS-96): HL-II assessment. IEEE Trans Power Syst 1998;13:171–6.
[27] Sinden G. Characteristics of the UK wind resource: long-term patterns and relationship to electricity demand. Energy Policy 2007;35:112–27.
[28] Elgerd IO. Electric energy system theory: an introduction. New York: McGraw-Hill, Inc.; 1971.
[29] Das D. A fuzzy multiobjective approach for network reconfiguration of distribution systems. IEEE Power Del 2006;21:202–9.
[30] Abu-Mouti FS, El-Hawary ME. Heuristic curve-fitted technique for distributed generation optimisation in radial distribution feeder systems. IET Gener Trans Distrib 2011;5:172–80.
[31] Jain N, Singh S, Srivastava S. A generalized approach for DG planning and viability analysis under market scenario. IEEE Ind Electron 2013;60:5075–85.
[32] Tsili M, Papathanassiou S. A review of grid code technical requirements for wind farms. IET Renew Power Gener 2009;3:308–32.